

Supplemental material for: Fundamental limits on the rate of bacterial cell division

Nathan M. Belliveau^{1, †}, Griffin Chure^{2, †}, Christina L. Hueschen³, Hernan G. Garcia⁴, Jane Kondev⁵, Daniel S. Fisher⁶, Julie A. Theriot^{1, 7}, Rob Phillips^{8, 9, *}

***For correspondence:**

[†]These authors contributed
equally to this work

¹Department of Biology, University of Washington, Seattle, WA, USA; ²Department of Applied Physics, California Institute of Technology, Pasadena, CA, USA; ³Department of Chemical Engineering, Stanford University, Stanford, CA, USA; ⁴Department of Molecular Cell Biology and Department of Physics, University of California Berkeley, Berkeley, CA, USA; ⁵Department of Physics, Brandeis University, Waltham, MA, USA; ⁶Department of Applied Physics, Stanford University, Stanford, CA, USA; ⁷Allen Institute for Cell Science, Seattle, WA, USA; ⁸Division of Biology and Biological Engineering, California Institute of Technology, Pasadena, CA, USA; ⁹Department of Physics, California Institute of Technology, Pasadena, CA, USA; *Address correspondence to phillips@pboc.caltech.edu

16 Contents

Table 1. Overview of proteomic data sets.

Author	Method	Reported Quantity
Taniguchi <i>et al.</i> (2010)	YFP-fusion, cell fluorescence	fg/copies per cell
Valgepea <i>et al.</i> (2012)	mass spectrometry	fg/copies per cell
Peebo <i>et al.</i> (2014)	mass spectrometry	fg/copies per fl
Li <i>et al.</i> (2014)	ribosomal profiling	fg/copies per cell ^a
Soufi <i>et al.</i> (2015)	mass spectrometry	fg/copies per cell
Schmidt <i>et al.</i> (2016)	mass spectrometry	fg/copies per cell ^b

a. The reported values assume that the proteins are long-lived compared to the generation time but are unable to account for post-translational modifications that may alter absolute protein abundances.

b. This mass spectrometry approach differs substantially from the others since in addition to the relative proteome-wide abundance measurements, the authors performed absolute quantification of 41 proteins across all growth conditions (see Section ?? for more details on this).

Summary of Proteome Data: Experimental Details

Here we provide a brief summary of the experiments behind each proteomic data sets. The purpose of this section is to better identify the steps taken by the authors to arrive at absolute protein abundances. In the following section (Section ??) we will then provide a summary of the final protein abundance measurements that were used for in the main text. Table ?? provides an overview of the main data sets that we considered. These are predominately mass spectrometry-based, with the exception of the work from Li *et al.* (2014) which used ribosomal profiling, and the fluorescence-based counting done in Taniguchi *et al.* (2010).

Fluorescence based measurements

In the work of ?, the authors used a chromosomal YFP fusion library where individual strains have a specific gene tagged with a YFP-coding sequence. 1018 of 1400 attempted strains were used in their work. For each strain, a fluorescence microscope was used to collect cellular YFP intensities. Through automated image analysis, the authors normalized intensity measurements by cell size to account for the change in size and expression variability across the cell cycle. YFP intensities were also corrected for cellular autofluorescence, and final absolute protein levels were determined by a calibration with single-molecule fluorescence intensities, performed separately using a purified YFP solution.

Ribosomal profiling measurements

The work of ? takes a sequencing based approach to estimate protein abundance. Ribosomal profiling, which refers to the deep sequencing of ribosome-protected mRNA fragments, provides a quantitative measurement of the protein synthesis rate. As long as the protein life-time is long relative to the cell doubling time, it is possible to also estimate absolute protein copy numbers.

To perform ribosomal profiling, ribosome-protected mRNA is extracted from cell lysate and selected on a denaturing polyacrylamide gel, and sequences are obtained by deep sequencing (15–45 nt long fragments collected and sequenced by using an Illumina HiSeq 2000 in ?). Counts of ribosome footprints from the sequencing data are corrected empirically for position-dependent biases in ribosomal density across each gene, as well as dependencies on specific sequences including the Shine-Dalgarno sequence. These data-corrected ribosome densities represent relative protein synthesis rates.

Absolute protein synthesis rates are obtained by multiplying the relative rates by the total cellular protein per cell. The total protein per unit volume was determined with the Lowry method to quantify total protein, calibrated against bovine serum albumin (BSA). By counting colony-forming

units following serial dilution of their cell cultures, they then calculated the total protein per cell. The absolute protein synthesis rate has units of proteins per generation, and for stable proteins will also correspond to the protein copy number per cell.

Mass spectrometry measurements

Unsurprisingly, the data is predominantly mass spectrometry based, largely due to the tremendous improvements in sensitivity of instruments over the last decade, as well as improvements in sample preparation and data analysis pipelines. It is now a relatively routine task to extract protein from a cell and quantify the majority of proteins by shotgun proteomics. In general, this involved lysing cells, enzymatically digesting the proteins into short peptide fragments, and then introducing them into the mass spectrometer (commonly employing liquid chromatography and electrospray ionization), which itself can have multiple rounds of detection and further fragmentation of the peptides.

Most quantitative experiments rely on labeling protein with stable isotopes, which allow multiple samples to be measured simultaneously by the mass spectrometer. By combining samples of known total protein abundance (i.e. one sample of interest, and one reference), it is possible to determine relative protein abundances. With relative protein abundances in hand, absolute protein abundances can be estimated following the same approach used above for ribosomal profiling, which is to multiply each relative abundance measurement by the total cellular protein per cell. This is the approach taken by ? and ?, with relative protein abundances determined based on the relative peptide intensities (label free quantification 'LFQ' intensities). For the data of ?, total protein per cell was determined by measuring total protein by the Lowry method, and counting colony-forming units following serial dilution. For the data from ?, the authors did not determine cell quantities and instead report the cellular protein abundances in protein per unit volume by assuming a mass density of 1.1 g/ml, with a 30% dry mass fraction.

A key distinction in the mass spectrometry work of ? is that in addition to determining relative abundance, they performed absolute quantification of 41 enzymes covering over four orders of magnitude in cellular abundance. Here, a synthetic peptide was generated for each of the 41 proteins, doped into each protein sample, and used to provide an calibration between measured mass spectrometry intensities and absolute protein abundances. These absolute measurements, determined for every growth condition considered in their work, were then used as a calibration curve to convert proteomic-wide relative abundances into absolute protein abundance per cell. A more extensive discussion of the ? data set can be found in Section ?? .

Summary of Proteomic Data

In ?? we show the coverage and overlap of all proteins quantified across each data set using an UpSet diagram (?).

Estimation of total protein, cell size, and surface area across all growth conditions.

In ?? we looked at a number of recent cell size measurements and potential issues with the values used by Schmidt *et al.*. Since most of the proteomic data sets lack cell size measurements, we chose instead to use a common set of size measurements for any analysis requiring cell size or surface area. Since each of the data sets used either K-12 MG1655 or its derivative, BW25113 (from the lab of Barry L. Wanner; the parent strain of the Keio collection (??)), we fit the MG1655 cell size data from Si *et al.* 2017, 2019 using the `optimize.curve_fit` function from the Scipy python package (?).

The size data is shown in Figure ??(A) and (B), for the cell length and width, respectively. The length data was well described by the exponential function $0.5 e^{1.09 \cdot \lambda} + 1.76 \mu\text{m}$, while the width data was well described by $0.64 e^{0.24 \cdot \lambda} \mu\text{m}$. In order to estimate cell size we take the cell as a cylinders

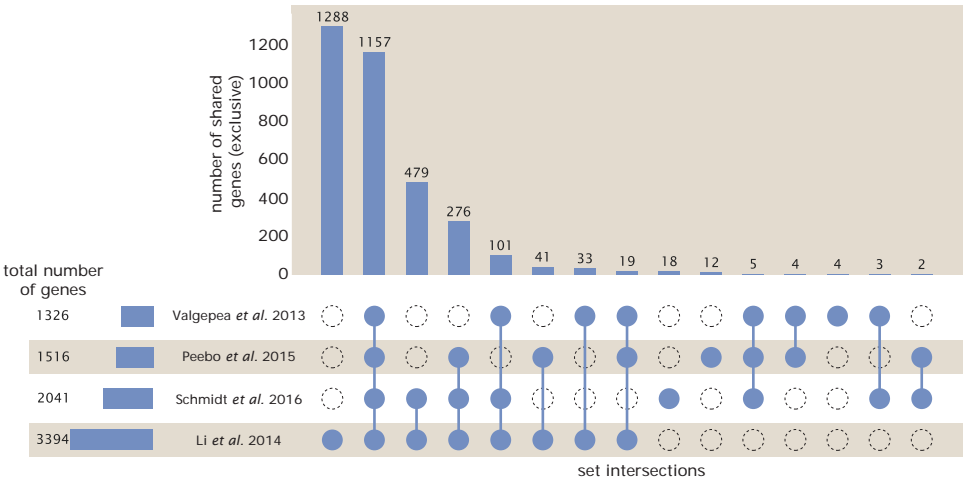


Figure 1. Comparison of proteomic coverage across different data sets.

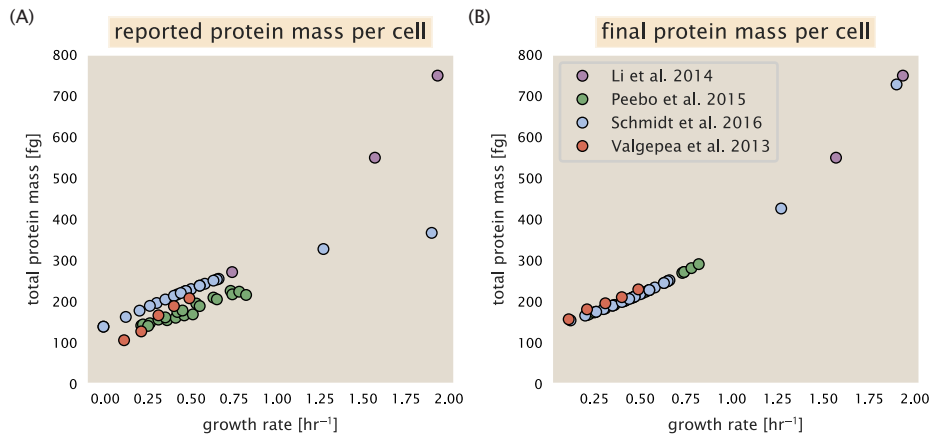


Figure 2. Summary of the growth-rate dependent total protein abundance for each data set.

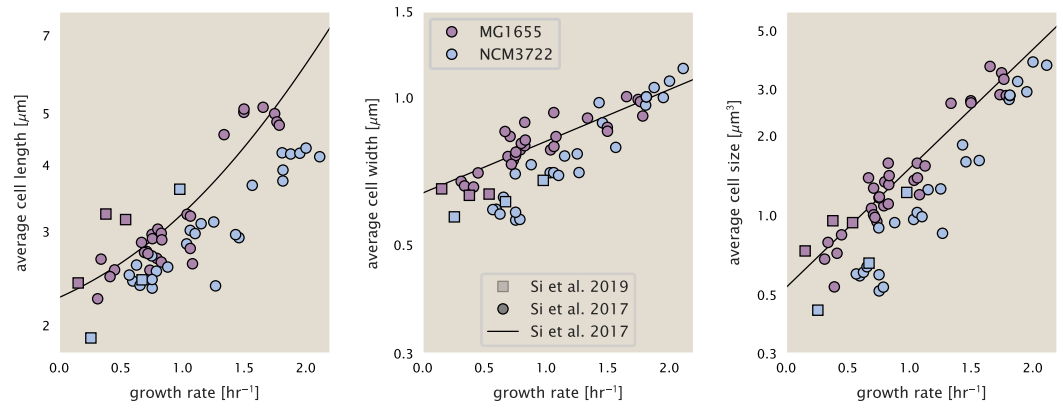


Figure 3. Summary of size measurements from Si *et al.* 2017, 2019. Cell lengths and widths were measured from cell contours obtained from phase contrast images, and refer to the long and short axis respectively. (A) Cell lengths and (B) cell widths show the mean measurements reported (they report 140-300 images and 5,000-30,000 for each set of samples; which likely means about 1,000-5,000 measurements per mean value reported here since they considered about 6 conditions at a time). Fits were made to the MG1655 strain data; length: $0.5 e^{1.09 \cdot \lambda} + 1.76 \mu\text{m}$, width: $0.64 e^{0.24 \cdot \lambda} \mu\text{m}$. (C) Cell size, V , was calculated as cylinders with two hemispherical ends (Equation ??). The MG1655 strain data gave a best fit of $0.533 e^{1.037 \cdot \lambda} \mu\text{m}^3$.

95 with two hemispherical ends (??). Specifically, cell size (or volume) is estimated from,

$$V = \pi \cdot r^2 \cdot (l - 2r/3), \quad (1)$$

96 where r is half the cell width. A best fit to the data is described by $0.533 e^{1.037 \cdot \lambda} \mu\text{m}^3$. Calculation of
97 the cell surface area is given by,

$$S = \eta \cdot \pi \left(\frac{\eta \cdot \pi}{4} - \frac{\pi}{12} \right)^{-2/3} V^{2/3}, \quad (2)$$

98 where η is the aspect ratio ($\eta = l/w$) (?).

99 Additional Considerations of Schmidt *et al.* Data Set

100 While the dataset from Schmidt *et al.* remains a heroic effort that our lab continues to return
101 to as a resource, there were steps taken in their calculation of protein copy number that we felt
102 needed some further consideration. In particular, the authors made an assumption of constant
103 cellular protein concentration across all growth conditions and used measurements of cell volume
104 that appear inconsistent with an expected exponential scaling of cell size with growth rate that is
105 well-documented in *E. coli* (???).

106 We begin by looking at their cell volume measurements, which are shown in blue in Figure
107 ??. As a comparison, we also plot cell sizes reported in three other recent papers: measurements
108 from Taheri-Araghi *et al.* and Si *et al.* come from the lab of Suckjoon Jun, while those from Basan
109 *et al.* come from the lab of Terence Hwa. Each set of measurements used microscopy and cell
110 segmentation to determine the length and width, and then calculated cell size by treating the cell
111 as a cylinder with two hemispherical ends. While there is a large discrepancy in cell size between the
112 two research groups, Basan *et al.* found that this came specifically from uncertainty in determining
113 the cell width, which is prone to inaccuracy given the small cell size and optical resolution limits
114 (further described in their supplemental text). Perhaps the more concerning point is that while
115 each of these alternative measurements show an exponential increase in cell size at faster growth
116 rates, the measurements used by Schmidt *et al.* appear to plateau. This resulted in an analogous
117 trend in their final reported total cellular protein per cell as shown in Figure ?? (purple data points),
118 and is in disagreement with other measurements of total protein at these growth rates (?).

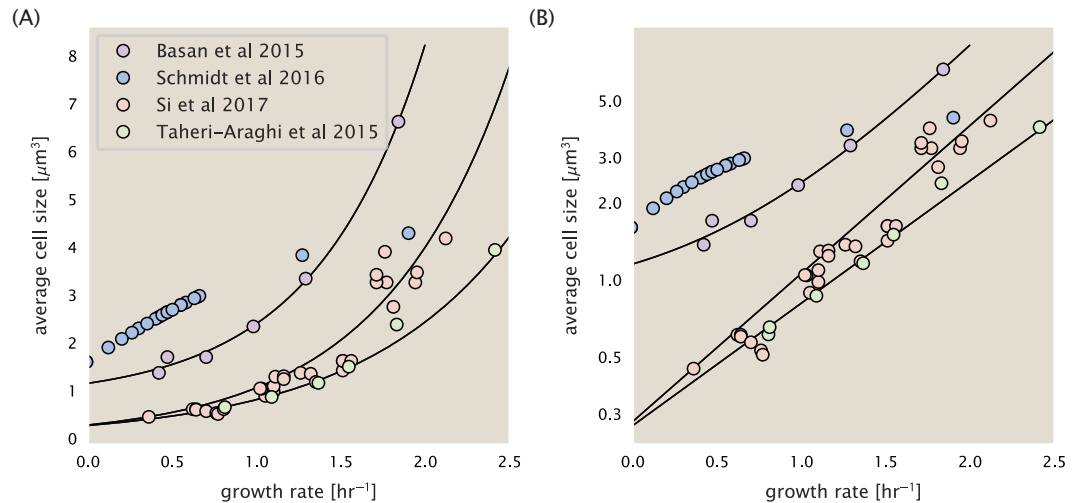


Figure 4. Measurements of cell size as a function of growth rate. (A) Plot of the reported cell sizes from several recent papers. The data in blue come from Volkmer and Heinemann, 2011 (?) and were used in the work of Schmidt *et al.*. Data from the lab of Terence Hwa are shown in red (?), while the two data sets shown in green and purple come from the lab of Suckjoon Jun (??). (B) Same as in (A) but with the data plotted on a logarithmic y-axis to highlight the exponential scaling that is expected for *E. coli*.

119 Since it is not obvious how measurements of cell size might have influenced their reported
 120 protein abundances, we will go through this calculation in the next section. We will also show
 121 how these can be adjusted to better reflect the alternative measurements of cell size shown in Figure
 122 ??. Finally, we consider several strategies to adjust the reported copy numbers, with the result
 123 summarized in Figure ??. For most growth conditions, we find that total protein expectations are
 124 not expected to change dramatically. However, for the fastest growth conditions, with glycerol +
 125 supplemented amino acids, and LB media, there is quite a bit of variability among the different
 126 estimates.

127 Effect of cell volume on reported absolute protein abundances

128 The authors calculated proteome-wide protein abundance by first determining absolute abun-
 129 dances of 41 pre-selected proteins, which relied on adding synthetic heavy reference peptides into
 130 their protein samples at known abundance (with proteins selected to cover the range of expected
 131 copy numbers). This absolute quantitation was performed in replicate for each growth condition.
 132 Separately, the authors also performed a more conventional mass spectrometry measurement
 133 for samples from each growth condition, which attempted to maximize the number of quantified
 134 proteins but only provided relative abundances based on peptide intensities. Finally, using their
 135 41 proteins with absolute abundances already determined, they then created calibration curves
 136 with which to relate their relative intensity to absolute protein abundance for each growth condi-
 137 tion. This allowed them to estimate absolute protein abundance for all proteins detected in their
 138 proteome-wide data set. Combined with their flow cytometry cell counts, they were then able to
 139 determine absolute abundance of each protein detected on a per cell basis.

140 While this approach provided absolute abundances, another necessary step needed to arrive at
 141 total cellular protein is to account for any protein loss during their various protein extraction steps.
 142 Here the authors attempted to determine total protein separately using a BCA protein assay. In
 143 personal communications, it was noted that determining reasonable total protein abundances by
 144 BCA across their array of growth conditions was particularly troublesome. Instead, they noted
 145 confidence in their total protein measurements for cells grown in M9 minimal media + glucose
 146 and used this as a reference point with which to estimate the total protein for all other growth

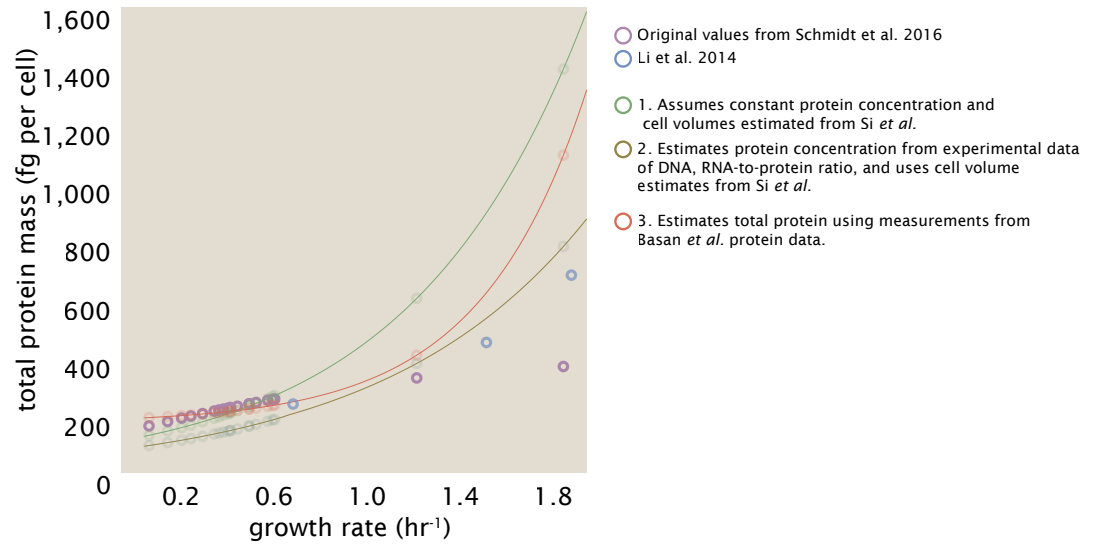


Figure 5. Alternative estimates of total cellular protein for the growth conditions considered in Schmidt et al. The original protein mass from Schmidt et al. and Li et al. are shown in purple and blue, respectively. *Green*: Rescaling of total protein mass assuming a growth rate independent protein concentration and cell volumes estimated from Si et al. 2017. *Gold*: Rescaling of total protein mass using estimates of growth rate-dependent protein concentrations and cell volumes estimated from Si et al. 2017. *Red*: Rescaling of total protein mass using the experimental measurements from Basan et al. 2015.

conditions.

For cells grown in M9 minimal media + glucose an average total mass of $M_p = 240$ fg per cell was measured. Using their reported cell volume, reported as $V_{orig} = 2.84$ fl, a cellular protein concentration of $[M_p]_{orig} = M_p / V_{orig} = 85$ fg/fl. Now, taking the assumption that cellular protein concentration is relatively independent of growth rate, they could then estimate the total protein mass for all other growth conditions from,

$$M_{p,i} = [M_p]_{orig} \cdot V_i \quad (3)$$

where $M_{p,i}$ represents the total protein mass per cell and V_i is the cell volume for each growth condition i as measured in Volkmer and Heinemann, 2011. Here the thinking is that the values of $M_{p,i}$ reflects the total cellular protein for growth condition i , where any discrepancy from their absolute protein abundance is assumed to be due to protein loss during sample preparation. The protein abundances from their absolute abundance measurements noted above were therefore scaled to their estimates and are shown in Figure ?? (purple data points).

If we instead consider the cell volumes predicted in the work of Si et al., we again need to take growth in M9 minimal media + glucose as a reference with known total mass, but we can follow a similar approach to estimate total protein mass for all other growth conditions. Letting $V_{Si_glu} = 0.6$ fl be the predicted cell volume, the cellular protein concentration becomes $[M_p]_{Si} = M_p / V_{Si_glu} = 400$ fg/fl. The new total protein mass per cell can then be calculated from,

$$M'_{p,i} = [M_p]_{Si} \cdot V_{Si,i} \quad (4)$$

where $M'_{p,i}$ is the new protein mass prediction, and $V_{Si,i}$ refers to the new volume prediction for each condition i . These are shown as [] dots in Figure ??.

Assumption of constant protein concentration across growth conditions

We next relax the assumption that cellular protein concentration is constant and instead, attempt to estimate it using experimental data. Here we first note that for across almost the entire range of growth rates considered here, protein, DNA, and RNA accounted for at least 90 % of the dry

mass in measurements from the lab of Terence Hwa (?). They also found that the total dry mass concentration was roughly constant across growth conditions. Under such a scenario, we can calculate the total dry mass concentration for protein, DNA, and RNA, which is given by $1.1 \text{ g/ml} \times 30\% \times 90\%$ or about $[M_p] = 300 \text{ fg per fl}$. Using the cell volume predictions from Si *et al.*, we can then calculate the associated mass per cell.

However, even if dry mass concentration is relatively constant across growth conditions, it is not a given that protein concentration should also be constant. In particular, we know that rRNA increases substantially at faster growth rates (?). This is a well-documented result that arises from an increase in the fraction of ribosomes at faster growth rates (?). To proceed we will use therefore rely on experimental measurements of total DNA content per cell that also come from Basan *et al.*, and RNA to protein ratios that were measured in Dai *et al.* (and cover the entire range of growth conditions considered here). These are reproduced in Figure ??(A) and (B), respectively.

Assuming that the protein, DNA, and RNA account for 90 % of the total dry mass, the protein mass can then determined by first subtracting the experimentally measured DNA mass, and then using the experimental estimate of the RNA to protein ratio. The total protein per cell is will be related to the summed RNA and protein mass by,

$$M_p = \frac{[M_p + M_{RNA}]}{1 + (RP_{ratio})}. \quad (5)$$

(RP_{ratio} refers to the RNA to protein ratio as measured by Dai *et al.*. In Figure ??(C) we plot the estimated cellular concentrations for protein, DNA, and RNA from these calculations, and in Figure ??(D) we plot their total expected mass per cell.

Estimating cellular protein concentration as a function of growth rate.

One of the challenges in our estimates in the preceding sections is the need to estimate protein concentration and cell volumes. These are inherently difficult to to accurately due to the small size of *E. coli*. Indeed, for all the additional measurements of cell volume included in Figure ??, no measurements were performed for cells growing at rates below 0.5 hr^{-1} . It therefore remains to be determined whether our extrapolated cell volume estimates are appropriate, with the possibility that the logarithmic scaling of cell size might break down for slower growth.

In our last approach we therefore attempt to estimate total protein using experimental data that required no estimates of concentration or cell volume. Specifically, in the work of Basan *et al.*, the authors measured total protein per cell for a broad range of growth rates (reproduced in Figure ??). These were determined by first measuring bulk protein from cell lysate, measured by the colorimetric Biuret method (?), and then abundance per cell was calculated from cell counts from either plating cells or a Coulter counter. While it is unclear why Schmidt *et al.* was unable to take a similar approach, the results from Basan *et al.* appear more consistent with our expectation that cell mass will increase exponentially with faster growth rates. In addition, although they do not consider growth rates below about 0.5 hr^{-1} , it is interesting to note that the protein mass per cell appears to plateau to a minimum value at slow growth. In contrast, our estimates using cell volume so far have predicted that total protein mass should continue to decrease slightly for slower growing cells. By fitting this data to an exponential function dependent on growth rate, we could then estimate the total protein per cell for each growth condition considered by Schmidt *et al.*. These are plotted in red in Figure ??.

Extending Estimates to a Continuum of Growth Rates

In the main text, we considered a standard stopwatch of 5000 s to estimate the abundance of the various protein complexes considered. In addition to point estimates, we also showed the estimate as a function of growth rate as transparent grey curves. In this section, we elaborate on this continuum estimate, giving examples of estimates that scale with either cell volume, cell surface area, or number of origins of replication.

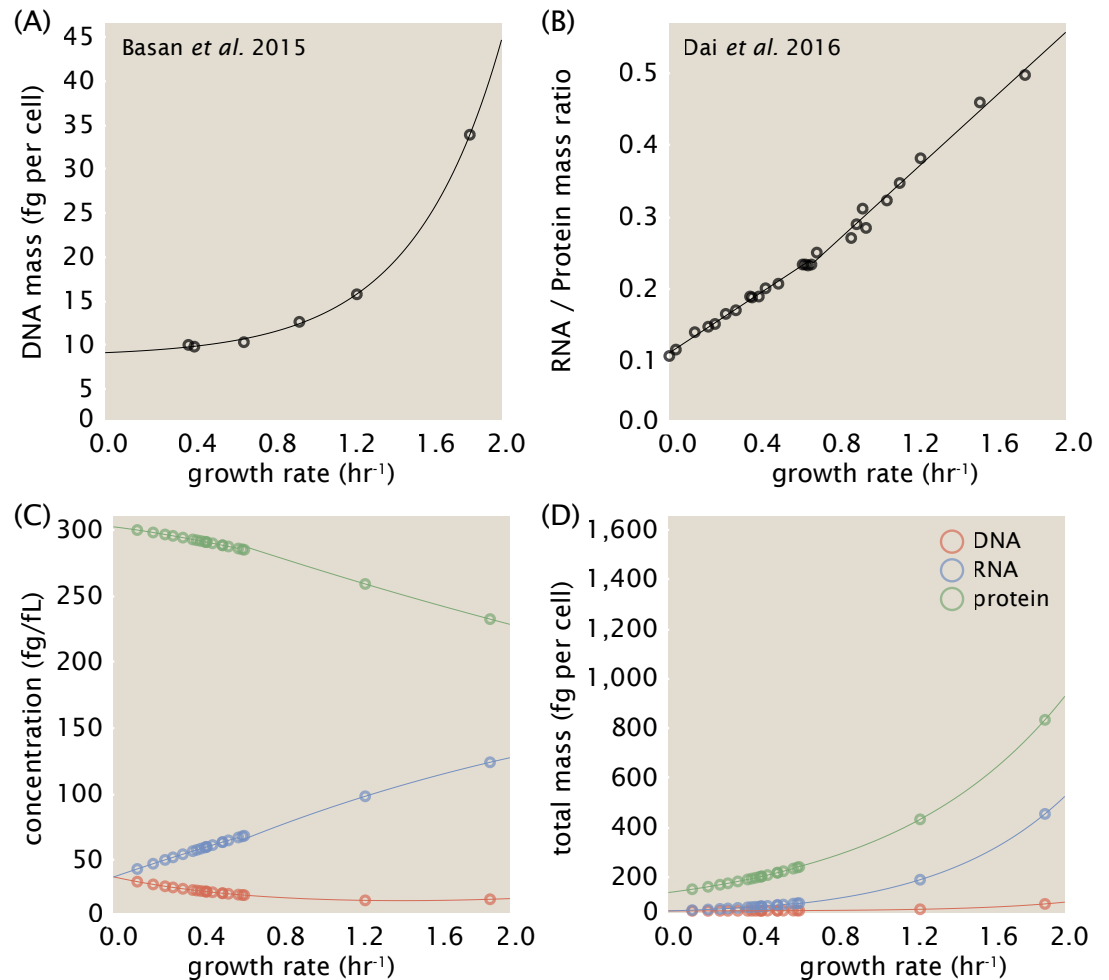


Figure 6. Empirical estimate of cellular protein, DNA, and RNA as a function of growth rate. (A) Measured DNA mass per cell as a function of growth rate, reproduced from Basan *et al.* 2015. The data was fit to an exponential curve (DNA mass in fg per cell is given by $0.42 e^{2.23 \cdot \lambda} + 7.2$ fg per cell, where λ is the growth rate in hr⁻¹). (B) RNA to protein measurements as a function of growth rate. The data was fit to two lines: for growth rates below 0.7 hr⁻¹, the RNA/protein ratio is given by $0.18 \cdot \lambda + 0.093$, while for growth rates faster than 0.7 hr⁻¹ the RNA/protein ratio is given by $0.25 \cdot \lambda + 0.035$. For (A) and (B) cells are grown under varying levels of nutrient limitation, with cells grown in minimal media with different carbon sources for the slowest growth conditions, and rich-defined media for fast growth rates. (C) Predictions of cellular protein, DNA, and RNA concentration. (D) Total cellular mass predicted for protein, DNA, and RNA using the cell size predictions from Si *et al.*

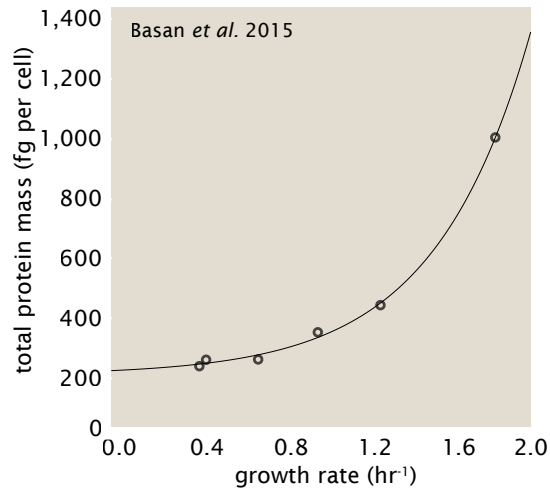


Figure 7. Total cellular protein reported in Basan *et al.* 2015. Measured protein mass as a function of growth rate as reproduced from Basan *et al.* 2015, with cells grown under different levels of nutrient limitation. The data was fit to an exponential curve where protein mass in fg per cell is given by $14.65 e^{2.180 \cdot \lambda} + 172$ fg per cell, where λ is the growth rate in hr^{-1} .

Estimation of the total cell mass

For many of the processes estimated in the main text we relied on a cellular dry mass of ≈ 300 fg from which we computed elemental and protein fractions using knowledge of fractional composition of the dry mass. At modest growth rates, such as the 5000 s doubling time used in the main text, this is a reasonable number to use as the typical cell mass is ≈ 1 pg and *E. coli* cells can be approximated as 70% water by volume. However, as we have shown in the preceding sections, the cell size and therefore cell volume is highly dependent on the growth rate. This means that a dry mass of 300 fg cannot be used reliably across all growth rates.

Rather, using the phenomenological description of cell volume scaling exponentially with growth rate, and using a rule-of-thumb of a cell buoyant density of ≈ 1.1 pg / fL (BNID: 103875), we can calculate the cell dry mass across a range of physiological growth rates as

$$m_{\text{cell}} \approx \rho V(\lambda) \approx \rho a e^{\lambda \cdot b} \quad (6)$$

where a and b are constants with units of μm^3 and hr , respectively. The value of these constants can be estimated from the careful volume measurements performed by ?, as is described in the previous section.

Complex Abundance Scaling With Cell Volume

Several of the estimates performed in the main text are implicitly dependent on the cell volume. This includes processes such as ATP synthesis and, most prominently, the transport of nutrients. Of the latter, we estimated the number of transporters that would be needed to shuttle enough carbon, phosphorus, and sulfur across the membrane to build new cell mass. To do so, we used elemental composition measurements combined with a 300 fg cell dry mass to make the point estimate. As we now have a means to estimate the total cell mass as a function of volume, we can generalize these estimates across growth rates.

Rather than discussing the particular details of each transport system, we will derive this scaling expression in very general terms. Consider we wish to estimate the number of transporters for some substance X , which has been measured to be make up some fraction of the dry mass θ_X . If we assume that, irrespective of growth rate, the cell dry mass is $\approx 30\%$ of the total cell mass, we can state that the total mass of substance X as a function of growth rate is

$$m_X \approx 0.3 \times \rho V(\lambda) \theta_X, \quad (7)$$

where we have used $\rho V(\lambda)$ as an estimate of the total cell mass, defined in ???. To convert this to the number of units N_X of substance X in the cell, we can use the formula weight w_X of a single unit of X in conjunction with ??,

$$N_X \approx \frac{m_X}{w_X}. \quad (8)$$

To estimate the number of transporters needed, we make the approximation that loss of units of X via diffusion through porins or due to the permeability of the membrane is negligible and that a single transporter complex can transport substance X at a rate r_X . As this rate r_X is in units of X per time per transporter, we must provide a time window over which the transport process can occur. This is related to the cell doubling time τ , which can be calculated from the growth rate λ as $\tau = \log(2)/\lambda$. Putting everything together, we arrive at a generalized transport scaling relation of

$$N_{\text{transporters}}(\lambda) = \frac{0.3 \times \rho V(\lambda) \theta_X}{w_X r_X \tau}. \quad (9)$$

This function is used to draw the continuum estimates for the number of transporters seen in Figures 2 and 3 as transparent grey curves. Occasionally, this continuum scaling relationship will not precisely agree with the point estimate outlined in the main text. This is due to the fact that we make an initial approximation made of a dry cell mass of ≈ 300 fg for the point estimate while we consider more precise values in the continuum estimate. We note, however, that both this scaling relation and the point estimates are meant to describe the order-of-magnitude observed, and not the predict the exact values of the abundances.

??? is a very general relation for processes where the cell volume is the "natural variable" of the problem. This means that, as the cell increases in volume, the requirements for substance X also scale with volume rather than scaling with surface area, for example. So long as the rate of the process, the fraction of the dry mass attributable to the substance, and the formula mass of the substance is known, ??? can be used to compute the number of complexes needed. For example, to compute the number of ATP synthases per cell, ??? can be slightly modified to the form

$$N_{\text{ATP synthases}}(\lambda) = \frac{0.3 \times \rho V(\lambda) \theta_{\text{protein}} N_{\text{ATP}}}{w_{AA} r_{\text{ATP}} \tau}, \quad (10)$$

where we have included the term N_{ATP} to account for the number of ATP equivalents needed per amino acid for translation (≈ 4 , BNID: 114971), and w_{AA} is the average mass of an amino acid. The grey curves in Figure 4 of the main text were made using this type of expression.

A Relation for Complex Abundance Scaling With Surface Area

In our estimation for the number of complexes needed for lipid synthesis and peptidoglycan maturation, we used a particular estimate for the cell surface area ($\approx 5 \mu m^2$, BNID: 101792) and the fraction of dry mass attributable to peptidoglycan ($\approx 3\%$, BNID: 101936). Both of these values come from glucose-fed *E. coli* in balance growth. As we are interested in describing the scaling as a function of the growth rate, we must consider how these values scale with cell surface area, which is the natural variable for these types of processes. In the coming paragraphs, we highlight how we incorporate a condition dependent surface area in to our calculation of the number of lipids and murein monomers that need to be synthesized and crosslinked, respectively.

Number of Lipids

To compute the number of lipids as a function of growth rate, we make the assumption that some features, such as the surface area of a single lipid ($A_{\text{lipid}} \approx 0.5 \text{ nm}^2$, BNID: 106993) and the total fraction of the membrane composed of lipids ($\approx 40\%$, BNID: 100078) are independent of the growth rate. Using these approximations combined with ??, and recognizing that each membrane is composed of two leaflets, we can compute the number of lipids as a function of growth rate as

$$N_{\text{lipids}}(\lambda) \approx \frac{4 \text{ leaflets} \times 0.4 \times \eta \pi \left(\frac{\eta \pi}{4} - \frac{\pi}{12} \right)^{-2/3} V(\lambda)^{2/3}}{A_{\text{lipid}}} \quad (11)$$

284 where η is the length-to-width aspect ratio and V is the cell volume.

285 Number of Murein Monomers

286 In calculation of the number of transpeptidases needed for maturation of the peptidoglycan, we
 287 used an empirical measurement that $\approx 3\%$ of the dry mass is attributable to peptidoglycan and that
 288 a single murein monomer is $m_{\text{murein}} \approx 1000$ Da. While the latter is independent of growth rate, the
 289 former is not. As the peptidoglycan exists as a thin shell with a width of $w \approx 10$ nm encapsulating
 290 the cell, one would expect the number of murein monomers scales with the surface area of this
 291 shell. In a similar spirit to our calculation of the number of lipids, the total number of murein
 292 monomers as a function of growth rate can be calculated as

$$N_{\text{murein monomers}}(\lambda) \approx \frac{\rho_{\text{pg}} w \eta \pi \left(\frac{\eta \pi}{4} - \frac{\pi}{12} \right)^{-2/3} V(\lambda)^{2/3}}{m_{\text{murein}}}, \quad (12)$$

293 where ρ_{pg} is the density of peptidoglycan.

294 Complex Abundance Scaling With Number of Origins

295 While the majority of our estimates hinge on the total cell volume or surface area, processes related
 296 to the central dogma, namely DNA replication and synthesis of rRNA, depend on the number of
 297 chromosomes present in the cell. As discussed in the main text, the ability of *E. coli* to parallelize the
 298 replication of its chromosome by having multiple active origins of replication at a given is critical to
 299 synthesize enough rRNA, especially at fast growth rates. Derived in ?? and reproduced in the main
 300 text, the average number of origins of replication at a given growth rate can be calculated as

$$\langle \# \text{ori} \rangle \approx 2^{t_{\text{cyc}} \lambda / \ln 2} \quad (13)$$

301 where t_{cyc} is the total time of replication and division. We can make the approximation that $t_{\text{cyc}} \approx$
 302 70 min, which is the time it takes two replisomes to copy an entire chromosome.

303 In the case of rRNA synthesis, the majority of the rRNA operons are surrounding the origin of
 304 replication. Thus, at a given growth rate λ , the average dosage of rRNA operons per cell D_{rRNA} is

$$D_{\text{rRNA}}(\lambda) \approx N_{\text{rRNA operons}} \times 2^{t_{\text{cyc}} \lambda / \ln 2}. \quad (14)$$

305 This makes the approximation that *all* rRNA operons are localized around the origin. In reality,
 306 the operons are some distance away from the origin, making ?? an approximation.

307 In the main text, we stated that at the growth rate in question, there is ≈ 1 chromosome per
 308 cell. While a fair approximation, ?? illustrates that is not precisely true, even at slow growth rates.
 309 In estimating the number of RNA polymerases as a function of growth rate, we consider that re-
 310 gardless of the number of rRNA operons, they are all sufficiently loaded with RNA polymerase such
 311 that each operon produces one rRNA per second. Thus, the total number of RNA polymerase as a
 312 function of the growth rate can be calculated as

$$N_{\text{RNA polymerase}}(\lambda) \approx L_{\text{operon}} D_{\text{rRNA}} \rho_{\text{RNA polymerase}}, \quad (15)$$

313 where L_{operon} is the total length of an rRNA operon (≈ 4500 bp) and $\rho_{\text{RNA polymerase}}$ is packing density
 314 of RNA polymerase on a given operon, taken to be 1 RNA polymerase per 80 nucleotides.